

Crossover between polariton and phonon local states and effects of anisotropy on the polariton states

Victor Podolsky

Department of Physics, Queens College of CUNY, Flushing, New York 11367

(Received 5 May 1998; revised manuscript received 12 January 1999)

We consider local polariton states that are composed from optical phonons and photons localized around atomic impurities. We evaluate a photon contribution into polariton states and investigate the impurity-strength-driven crossover between polariton and phonon local states. The polariton states exhibit a macroscopic spatial size and the absence of the localization threshold. These features are attributed to a negative phonon dispersion, which leads to a nonstandard polariton density of states (DOS). We show that the DOS diverges at the bottom of the polariton gap in an isotropic medium, and it tends to a finite limit in anisotropic polar crystals. This leads to a thresholdless dependence of the frequency of the local state on the impurity strength in both cases. [S0163-1829(99)08337-X]

I. INTRODUCTION

Theoretical and experimental investigation of photon localization is one of the most active areas in condensed matter physics. The search for this phenomenon was originally restricted to strongly scattering disordered media.¹⁻⁵ It was later proposed that the defect-induced local photon states can exist in photonic crystals.⁶⁻⁸ A possibility of photon localization in regular crystals with atomic defects and the concept of local polariton states were introduced in Refs. 9 and 10. Considering a dipole-active impurity in a frequency-dispersive medium, authors discovered photon-atom bound states that present the coherently coupled atomic excitations and medium polaritons. When intra-atom transition frequencies fall inside the polariton gap, the radiative relaxation of the bound states is suppressed, and the induced field remains localized around the impurity. Using the Bethe-ansatz technique, the authors constructed a complete set of the scattering and bound states and investigated the polariton-impurity band in a system with spatially correlated impurities.

A theory of local polariton states has received development in Ref. 11. There were considered phonon-polariton states associated with the well-known local phonon states.^{12,13} It was shown that a negative phonon dispersion has a surprisingly drastic effect on new states. Unlike the pure phonon states, there is no lower critical value of the impurity strength that must be exceeded for the local polariton state to arise. It was also shown that near the bottom of the polariton gap the localization radius is macroscopically large, which supports the long-wavelength approximation used in Ref. 11. In Ref. 14, we analyzed effects of impurity-induced variations of elastic constants on the local states. Solving microscopic equations of motion in the long-wavelength limit, we found several local states of different symmetry. All new states split off the bottom of the polariton gap upon infinitesimally small increments of the impurity strength. This feature of the polariton states was attributed to the long-wavelength singularity of the density of states (DOS) at the bottom of the gap.

Local polariton states present the well-known phonon

states with the field corrections taken into account. A field contribution into these states decreases as the impurity strength increases and they move away from the bottom of the gap. In the present paper we investigate such an ‘‘impurity-strength-driven’’ crossover between polariton and phonon local states. Their long-wavelength nature allows us to analyze the crossover in the isotropic medium approximation. We show that the crossover takes place within a narrow frequency interval near the bottom of the polariton gap. However, despite the small size of the crossover region, the photon-phonon coupling sets a limit on the width of the spectral gap, allowing the same type of local states in the entire gap. We estimate the critical width and show that, in the case of the isotopic defects in ‘‘narrow’’ gaps, only light impurities can support local states.

The singularity of the DOS is provided by the long-wavelength polaritons and is generic for the isotropic model with negative phonon dispersion. We show that weak crystal anisotropy removes the singularity from the band boundary; however, it does not lead to a finite threshold for the local polariton states. At the same time, the crystal anisotropy turns the power-law relation between the impurity strength and the separation of the local state from the band boundary into the logarithmic relation.

II. LOCAL POLARITON STATES

Let us consider a dipole-active medium with an embedded impurity. Dynamical equations of the medium can be introduced phenomenologically or derived from the microscopic lattice equations in a polar crystal. In the latter case the displacements of ions within each elementary cell must be first expressed via the dipole moment of a cell, the displacement of its center of mass, and other similar variables, then the long-wavelength limit must be worked out. In the optical excitations sector, this leads to a model of coupled dipole oscillators (assigned to elementary cells), where the coupling determines the effective dynamical matrix of the crystal. This matrix is a second rank tensor depending on coordinates of oscillators. In the long-wavelength limit, due to a short-range (between neighboring oscillators) coupling, the dy-

namical matrix transforms into a local differential operator $\hat{\Omega}^2(\mathbf{r})$. A defect modifies the dynamical matrix $\hat{\Omega}^2(\mathbf{r}) \rightarrow \hat{\Omega}^2(\mathbf{r}) + \alpha \delta(\mathbf{r} - \mathbf{r}_0)$, where parameter α is the ‘‘strength’’ of the defect, and \mathbf{r}_0 is its coordinate. The resultant equations describe coupled electromagnetic and polarization waves (optical phonons) in a medium where dielectric permeability has a pointlike singularity:

$$[\omega^2 - \hat{\Omega}^2(\mathbf{k})] \mathcal{P}_{\mathbf{k}} = -\frac{d^2}{4\pi} \mathbf{E}_{\mathbf{k}} + \alpha \frac{a^3}{V} \mathcal{P}(\mathbf{0}), \quad (1)$$

$$(\omega^2 - c^2 k^2) \mathbf{E}_{\mathbf{k}} = -4\pi [(\omega^2 - c^2 k^2) \hat{\mathbf{P}}_{\parallel} + \omega^2 \hat{\mathbf{P}}_{\perp}] \mathcal{P}_{\mathbf{k}}. \quad (2)$$

Here $\mathcal{P}_{\mathbf{k}}$ and $\mathbf{E}_{\mathbf{k}}$ are Fourier components of the polarization and electric fields, $\hat{\Omega}^2(\mathbf{k})$ is the dynamical matrix of the medium, $\hat{\mathbf{P}}_{\parallel}$ and $\hat{\mathbf{P}}_{\perp}$ are the longitudinal and transverse projectors in \mathbf{k} representation, a is the lattice parameter, V is a volume of a sample, $d^2 = 4\pi q^2 / \mu a^3$ is the coupling parameter, and $\mathcal{P}(\mathbf{0}) = \sum_{\mathbf{k}} \mathcal{P}_{\mathbf{k}}$, where vectors \mathbf{k} belong to the first Brillouin zone.

Equation (1) implies that the impurity itself is not dipole active and it provides only local, extended over a distance of an order of the lattice parameter, distortion of the crystal. This is incorporated in equations via the inhomogeneous term of the dynamical matrix. Such structureless point like defects correspond to isotopes and dopants that chemically resemble the host ions. In this case the defect strength can be expressed as $\alpha = \omega'^2 \delta\gamma / \gamma - \omega'^2 \delta\mu / \mu$, where μ and γ are the reduced mass of the elementary cell and the elastic constant of the nearest-neighbors interaction, $\delta\mu$ and $\delta\gamma$ are their impurity-induced variations, and ω'^2 is the characteristic frequency depending on properties of the defect and the crystal.

In the isotropic approximation, the dynamical matrix can be presented as follows:

$$\hat{\Omega}^2 = \Omega_{\parallel}^2(k) \hat{\mathbf{P}}_{\parallel} + \Omega_{\perp}^2(k) \hat{\mathbf{P}}_{\perp}, \quad (3)$$

where $\Omega_{\parallel}^2(k)$ and $\Omega_{\perp}^2(k)$ are frequencies of the longitudinal and transverse phonons, respectively. Below we assume negative dispersion in the phonon branches, so they have the following long-wavelength asymptotes:

$$\Omega_{\perp}^2(k) \approx \Omega_0^2 - v_{\perp}^2 k^2, \quad (4)$$

$$\Omega_{\parallel}^2(k) \approx \Omega_0^2 - v_{\parallel}^2 k^2, \quad (5)$$

where the parameters v_{\perp} and v_{\parallel} set the ranges of the typical phonon velocities. Due to symmetry reasons, both phonon branches have the same activation frequency Ω_0 . For the ‘‘order of a magnitude’’ estimates we assume $v_{\perp} \sim v_{\parallel} \sim 10^2$ m/s, and $\Omega_0 \sim v/a \sim d$.

Solving Eqs. (1)–(3), one can obtain the spectral equation

$$1 = \frac{\alpha}{3} \left(\frac{a}{2\pi} \right)^3 \int d\mathbf{k} \left[(\omega^2 - \Omega_{\parallel}^2 - d^2)^{-1} + 2 \left(\omega^2 - \Omega_{\perp}^2 - \frac{d^2 \omega^2}{\omega^2 - c^2 k^2} \right)^{-1} \right] = \alpha I(\omega^2), \quad (6)$$

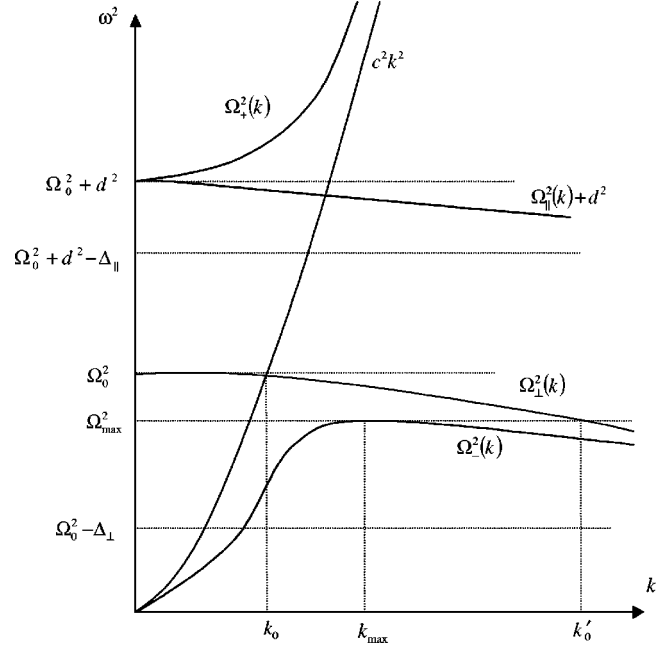


FIG. 1. Phonon and polariton dispersion curves. In this picture, Ω_{\pm} denote two polariton branches, Ω_{\parallel} and Ω_{\perp} are longitudinal and transverse phonon branches, Ω_0 is the optical phonon activation frequency, $\Omega_{\max}^2 = \Omega_0^2 - \Delta_{\parallel}$, Δ_{\parallel} , Δ_{\perp} denote the widths of the phonon bands, k_0 is the crossing-resonance momentum, and k'_0 is defined by the equation $\Omega_{\perp}^2(k'_0) = \Omega_1^2$.

where the integration is extended over the first Brillouin zone.

This equation defines spectra of all extended and local excitations. The dispersion relations of the extended states are determined by the poles of the integrand in Eq. (6). In the isotropic medium, there is a single longitudinal branch $\omega^2 = \Omega_{\parallel}^2 + d^2$, whereas the transverse band contains two polariton branches (Fig. 1):

$$\Omega_{\pm}(k) = \frac{1}{2} \left[\sqrt{(\Omega_{\perp} + ck)^2 + d^2} \pm \sqrt{(\Omega_{\perp} - ck)^2 + d^2} \right]. \quad (7)$$

The lower branch $\Omega_{-}(k)$ is activationless and nonmonotonic. Its ‘‘short-wavelength’’ asymptote,

$$\Omega_{-}(k) \approx \Omega_{\perp}(k) \left(1 - \frac{d^2}{2c^2 k^2} \right), \quad (8)$$

shows that the lower branch reaches its maximum at the point

$$k_{\max} \approx \left(\frac{2d\Omega_0}{v_{\perp} c} \right)^{1/2} \sim \beta^{1/2} a^{-1}. \quad (9)$$

Since $vk_{\max} \sim \beta^{1/2} \Omega_0 \ll \Omega_0$ and $ck_{\max} \sim \beta^{-1/2} \Omega_0 \gg \Omega_0$, the maximum of $\Omega_{-}(k)$ is located in the long-wavelength region but far away from the crossing-resonance point. Using Eqs. (7) and (8) one can find

$$\Omega_{\max}^2 = \Omega_0^2 - \Delta_1 \approx \Omega_0^2 - 2\beta d \Omega_0. \quad (10)$$

The polariton branches are separated by the gap, which extends from Ω_{\max}^2 to $\Omega_0^2 + d^2$. However, because the lon-

gitudinal band overlaps the top part of the polariton gap, the true spectral gap is between Ω_{\max}^2 and the minimum of the longitudinal branch $\Omega_{\min}^2 = \Omega_0^2 + d^2 - \Delta_{\parallel}$. The spectral gap is open only if the width of the polariton gap $d^2 + \Delta_{\perp}$ exceeds the width of the longitudinal band Δ_{\parallel} . Further, below we assume this and consider only local states inside the gap.

The frequency of the local state can be found from Eq. (6). Function $I(\omega^2)$ in this equation presents a sum of the ‘‘longitudinal’’ and ‘‘transverse’’ terms $I_{\parallel}(\omega^2)$ and $I_{\perp}(\omega^2)$. The transverse integral can be rewritten in the form

$$I_{\perp}(\omega^2) = \frac{2}{3} \left(\frac{a}{2\pi} \right)^3 \int \frac{(\omega^2 - c^2 k^2) d\mathbf{k}}{(\omega^2 - \Omega_{+}^2)(\omega^2 - \Omega_{-}^2)}. \quad (11)$$

When ω tends to Ω_{\max} , this integral diverges at the surface $\mathbf{k}^2 = k_{\max}^2$ due to the second factor in the denominator of the integrand. The transverse term dominates in $I(\omega^2)$ near the bottom of the gap, and a region of the Brillouin zone where $k \sim k_{\max}$ gives the major contribution into $I_{\perp}(\omega^2)$. As it follows from Eqs. (4), (7), and (9), in this region we can approximate

$$\Omega_{-}^2(k) \approx \Omega_{\max}^2 - 4v_{\perp}^2(k - k_{\max})^2. \quad (12)$$

It allows us to calculate $I(\omega^2)$ and determine the frequency of the local state

$$\sqrt{\omega^2 - \Omega_{\max}^2} \approx \frac{\alpha a}{3\pi v_{\perp}} (ak_{\max})^2 \sim \alpha \Omega_0^{-1} \beta. \quad (13)$$

In order to evaluate the localization radius of this state we consider the spatial distribution of the electric and polarization fields. Solving Eqs. (1) and (2), we obtain

$$\mathbf{E}(\mathbf{r}) = -\frac{\alpha a^3}{2\pi^2} \int d\mathbf{k} \exp(i\mathbf{k}\mathbf{r}) \left[\frac{\hat{\mathbf{P}}_{\parallel}}{\omega^2 - \Omega_{\parallel}^2 - d^2} + \frac{\omega^2 \hat{\mathbf{P}}_{\perp}}{(\omega^2 - \Omega_{+}^2)(\omega^2 - \Omega_{-}^2)} \right] \mathcal{P}(0). \quad (14)$$

Taking into account that the transverse field dominates in $\mathbf{E}(\mathbf{r})$, and the integral defining $\mathbf{E}_{\perp}(\mathbf{r})$ builds up near the surface $\mathbf{k}^2 = k_{\max}^2$, one can find the far-field asymptotes

$$\mathbf{E}(\mathbf{r}) \approx 4\pi \frac{\Omega_0^2}{c^2 k_{\max}^2} \mathcal{P}(r), \quad (15)$$

$$\mathcal{P}(r) \approx \{ \mathbf{n} \times [\mathbf{n} \times \mathcal{P}(0)] \} \frac{\sin(rk_{\max}) \exp(-r\kappa)}{rk_{\max}}, \quad (16)$$

where \mathbf{n} is a unitary radial vector, and

$$\kappa = \left(\frac{\omega^2 - \Omega_{\max}^2}{4v_{\perp}^2} \right)^{1/2} \approx \frac{\alpha a}{6\pi v_{\perp}} (ak_{\max})^2 \sim \beta \alpha \Omega_0^{-2} a^{-1} \quad (17)$$

is the inverse localization radius of the considered state.

III. CROSSOVER BETWEEN POLARITON AND PHONON LOCAL STATES

The distinct features of the local states near the bottom of the gap can be attributed to the singularity of the density of states in the lower polariton band. Since $\Omega_{-}^2(k)$ reaches its maximum at a surface of a finite area, the DOS diverges at Ω_{\max}

$$\rho(\omega^2) \approx \frac{a(ak_{\max})^2}{(2\pi)^2 v_{\perp}} (\Omega_{\max}^2 - \omega^2)^{-1/2}. \quad (18)$$

This singularity is provided by long-wavelength ($k \sim k_{\max}$) polaritons, which also dominate in the local states near the bottom of the gap. It explains the macroscopic sizes of the coherence length $l_{\text{coh}} = k_{\max}^{-1} \sim a\beta^{-1/2}$ and localization radius $l_{\text{loc}} = \kappa^{-1} \sim a\beta^{-1}$.

Local polariton states provide a possibility of a ‘‘phonon assisted’’ localization of optical photons in regular crystals. However, because k_{\max} is located far away from the crossing-resonance point ($k_{\max} \gg k_0$), the phonon content of the local states greatly exceeds their photon content. This can be illustrated by direct comparison of the mechanical and electromagnetic energy of the local state

$$W_{\text{phon}} = \frac{2\pi V}{d^2} \sum_{\mathbf{k}} \mathcal{P}_{\mathbf{k}}(\omega^2 + \hat{\mathbf{P}}^2) \mathcal{P}_{\mathbf{k}}, \quad (19)$$

$$W_{\text{phot}} = \frac{V}{8\pi} \sum_{\mathbf{k}} \mathbf{E}_{\mathbf{k}}^2 + \mathbf{H}_{\mathbf{k}}^2. \quad (20)$$

Straightforward but lengthy calculations based on equations and approximations discussed in the previous section lead to the estimate,

$$\frac{W_{\text{phot}}}{W_{\text{phon}}} \approx \left(\frac{d}{ck_{\max}} \right)^2 \sim \beta. \quad (21)$$

It is also worth mentioning that, in accordance with the relationship between the field amplitudes, $|\mathbf{H}_{\mathbf{k}}| = |\mathbf{k} \times \mathbf{E}_{\mathbf{k}}| c / \omega \approx |\mathbf{E}_{\mathbf{k}}| k_{\max} / k_0$, the magnetic part dominates in electromagnetic energy of the local state.

The position of the local level inside the spectral gap depends on a value of the defect strength α , which we consider below as an adjustable parameter. As Eq. (13) shows, local polariton states appear first at the bottom of the gap for $\alpha = +0$ and move inside the gap upon increasing the defect strength. This weakens the photon content of the local states and transforms them into the ordinary phonon states. In order to investigate this crossover, we need to evaluate $I(\omega^2)$ in the entire spectral gap. Away from the bottom of the gap, both terms of Eq. (6), $I_{\parallel}(\omega^2)$ and $I_{\perp}(\omega^2)$, become comparable, and calculations here require knowledge of the phonon dispersion laws in the entire Brillouin zone. Such information is not consistent with the approximations employed in our model, since in the short-wavelength region a crystal anisotropy cannot be neglected, and ion displacements within elementary cells must be considered in all details. However, we proceed with calculations assuming that the crossover takes place near the bottom of the gap. Noting that the details of the phonon dispersion can be incorporated into

the DOS in the phonon bands, we rely on a simple approximation accounting for Kohn's singularities at the band boundaries only

$$\rho_{\text{phon}}(\varepsilon) = \frac{8}{\pi \Delta_{\text{phon}}^2} \sqrt{(\varepsilon - \omega_{\text{min}}^2)(\omega_{\text{max}}^2 - \varepsilon)}, \quad (22)$$

where Δ_{phon} is the width of the phonon band, and ω_{min}^2 and ω_{max}^2 are the band boundaries.

In order to calculate $I_{\parallel}(\omega^2)$ in Eq. (6), we transform it into the integral over the longitudinal band

$$I_{\parallel}(\omega^2) = \frac{1}{3} \left(\frac{a}{2\pi} \right)^3 \int \frac{d\mathbf{k}}{\omega^2 - \Omega_{\parallel}^2 - d^2} = \frac{1}{3} \int_{\Omega_{\text{min}}^2}^{\Omega_{\text{min}}^2 + \Delta_{\parallel}} \frac{\rho_{\parallel}(\varepsilon) d\varepsilon}{\omega^2 - \varepsilon}, \quad (23)$$

where $\Omega_{\text{min}}^2 = \Omega_0^2 + d^2 - \Delta_{\parallel}$. Using Eq. (22) for $\rho_{\parallel}(\varepsilon)$ one can obtain

$$I_{\parallel}(\omega^2) = -\frac{4}{3\Delta_{\parallel}^2} (\sqrt{\Omega_{\text{min}}^2 + \Delta_{\parallel} - \omega^2} - \sqrt{\Omega_{\text{min}}^2 - \omega^2})^2. \quad (24)$$

The transverse integral has a similar form for $\omega \gg \Omega_{\text{max}}$, far away from the bottom of the gap (Appendix):

$$I_{\perp}(\omega^2) \approx \frac{8}{3\Delta_{\perp}^2} (\sqrt{\omega^2 + \Delta_{\perp} - \Omega_0^2} - \sqrt{\omega^2 - \Omega_0^2})^2. \quad (25)$$

In the opposite limit, for $\omega \gtrsim \Omega_{\text{max}}$, the transverse integral has the following singularities:

$$I_{\perp}(\omega^2) \approx \frac{8\Delta_{\perp}}{3\Delta_{\perp}^{3/2}} (\omega^2 - \Omega_{\text{max}}^2)^{-1/2} - \frac{16\Delta_{\perp}^{1/2}}{3\pi\Delta_{\perp}^{3/2}} \ln \left(\frac{\omega^2 - \Omega_{\text{max}}^2}{\Delta_{\perp}} \right). \quad (26)$$

Equations (22)–(24) allow us to consider the local levels anywhere in the gap. Since the corresponding local states present the superpositions of all normal modes of a pure crystal, we can qualitatively describe composition of the states comparing contributions into $I(\omega^2)$ from different parts of the Brillouin zone and different bands.

As we showed above, function $I(\omega^2)$ has a singularity at the bottom of the gap caused by the long-wavelength ($k \sim k_{\text{max}}$) polaritons. They also give the major contribution into $I(\omega^2)$ inside the interval, $\Omega_{\text{max}} < \omega \leq \Omega_0$. However, even for $\omega = \Omega_0$, their contribution is substantially weakened

$$I_{\perp}(\Omega_0^2) = \frac{8}{3\Delta_{\perp}} [1 + \mathcal{O}(\beta^{1/2})], \quad (27)$$

where the leading term is provided by the short-wavelength polaritons that are indistinguishable from transverse-optical phonons.

Outside the interval $\Omega_{\text{max}} \leq \omega \leq \Omega_{\text{max}} + \Delta_{\perp}/\Omega_{\text{max}}$, function $I(\omega^2)$ has a ‘‘phonon’’ structure. All terms related to the polariton singularity are weakened by power factors of a small parameter $\Delta_{\perp}/\Delta_{\perp} \sim \beta$. At the upper boundary of the gap we obtain

$$I(\Omega_{\text{min}}^2) = \frac{8}{3\Delta_{\parallel}^2} \left[\left(\frac{\sqrt{x+y} - \sqrt{y}}{x} \right)^2 - \frac{1}{2} \right] + \mathcal{O}(\beta^{1/2}), \quad (28)$$

where $x = \Delta_{\perp}/\Delta_{\parallel}$ and $y = d^2/\Delta_{\parallel} - 1$.

The value of $I(\Omega_{\text{min}}^2)$ determines the upper limit of the defect strength, which still allows the local state. Analysis shows that $I(\Omega_{\text{min}}^2)$ is positive if the width of the spectral gap $d^2 - \Delta_{\parallel}$ is below a certain limit,

$$d^2 - \Delta_{\parallel} \leq (\Delta_{\parallel}/8)(2 - \Delta_{\perp}/\Delta_{\parallel})^2. \quad (29)$$

Recalling that $I(\Omega_{\text{max}}^2) = +\infty$, we can conclude that only in ‘‘narrow’’ gaps are all local states associated with impurities of the same type. In the case of isotopes, the local states are supported by light impurities only. However, when $d^2 - \Delta_{\parallel}$ is greater than the critical value given by Eq. (29), the states near the bottom and the top of the gap are associated with different types of defects. For isotopes, these would be light and heavy impurities, respectively. The frequency regions of the corresponding states are limited inside the gap. The upper frequency for ‘‘light’’ states and the lower frequency for ‘‘heavy’’ ones can be found from equations, $\omega^2 I(\omega^2) = 1$ and $I(\omega^2) = 0$, respectively.

IV. EFFECT OF THE CRYSTAL ANISOTROPY ON THE LOCAL STATES

The considered above impurity-induced local states arise at the bottom of the polariton gap for infinitesimally small values of the impurity strength. This is in contrast with three-dimensional phonon systems where a lower threshold for local states (α_{min}) always exists. A general theorem regarding the finite threshold for local states in band gaps was given in Ref. 15. However, the proof of the theorem implies that the DOS vanishes at the band boundaries.

In our model, the absence of the threshold is caused by the singularity of the DOS $\rho(\omega^2) \propto (\Omega_{\text{max}}^2 - \omega^2)^{-1/2}$, which is provided by long-wavelength polaritons and is generic for any dipole-active phonon mode with negative dispersion and isotropic spectrum. Such long-wavelength modes can exist in cubic crystals; however, even weak crystal anisotropy removes the singularity from the bottom of the gap. In a cubic crystal, the anisotropic terms appear beyond the quadratic approximation of the phonon dispersion

$$\Omega_{\perp}^2(\mathbf{k}) = \Omega_0^2 - v_{\perp}^2 k^2 + \chi \Omega_0^2 (ak)^4 F(\hat{\mathbf{k}}), \quad (30)$$

where χ is the small parameter, and $F(\hat{\mathbf{k}})$ is some anisotropic function. The anisotropic term, as one can derive from Eq. (8), makes the position (k_{max}) and the value of the maximum in the lower polariton branch (Ω_{max}^2) dependent on the crystallographic direction. In the case of a weak anisotropy, the first effect can be neglected, and $\Omega_{\perp}^2(\mathbf{k})$ can be approximated near the surface $\mathbf{k}^2 = k_{\text{max}}^2$ as follows:

$$\Omega_{\perp}^2(\mathbf{k}) \approx \Omega_{\text{max}}^2 [1 + \chi F(\hat{\mathbf{k}})(ak_{\text{max}})^4] - 4v^2(k - k_{\text{max}})^2. \quad (31)$$

A small magnitude of the anisotropic term,

$$|\chi F(\hat{\mathbf{k}})(ak_{\text{max}})^4| \sim \chi \beta^2, \quad (32)$$

allows us to evaluate the asymptote of the DOS near the band boundary

$$\rho(\omega^2) \propto \oint_{\Omega_-(\mathbf{k})=\omega} d\sigma |\nabla_{\mathbf{k}} \Omega_-^2(\mathbf{k})|^{-1} \propto (\Omega_{\max}^2 - \omega^2 + A)^{-1/2}, \quad (33)$$

where $A \sim \chi \Omega_{\max}^2 (ak_{\max})^4 \langle F \rangle$, and $\langle F \rangle \sim 1$ is the angular average of the anisotropic function.

The crystal anisotropy removes the singularity of the DOS from the bottom of the gap because it destroys the degenerated global maximum of the polariton spectrum. There are many other physical factors that help to wash this singularity out, such as a lattice inharmoniously, electron-phonon interaction, thermal fluctuations, and so on. However, it seems unlikely that these factors can lower the DOS at the bottom of the gap from infinity to zero. On the other hand, it turns out that as long as the DOS has a nonzero finite value at the bottom of the gap, the local polariton states near the bottom have zero threshold and macroscopic localization radius.

Indeed, the equation defining the frequency of the local polariton state has a form

$$1 \approx \alpha \int_{\Omega_0^2 - \Delta_{\perp}}^{\Omega_{\max}^2} \frac{f(\varepsilon, \omega) \rho(\varepsilon) d\varepsilon}{\omega^2 - \varepsilon} = \alpha I(\omega^2), \quad (34)$$

where $\rho(\varepsilon)$ is the DOS, and the factor $f(\varepsilon, \omega)$ has absorbed the integration over \mathbf{k} directions and is regular and nonzero at the band boundaries. The singularity of the DOS, if there is any, helps us make a fast evaluation of the leading term ($[(\omega - \Omega_{\max})]^{-1/2}$ singularity) of $I(\omega^2)$ near Ω_{\max}^2 . However, it is clear that unless the DOS tends to zero at the band boundary, $I(\omega^2)$ always has a (loglike) singularity. For instance, accounting for weak anisotropy only, one can obtain

$$1 \approx -\alpha \frac{a(ak_{\max})^2}{3\pi^2 v_{\perp} A^{1/2}} \ln \left(\frac{\omega^2 - \Omega_{\max}^2}{A} \right). \quad (35)$$

This equation is valid near the band boundary ($\omega^2 - \Omega_{\max}^2 \ll A$), and it explicitly shows that α tends to zero when the local state approaches the bottom of the gap.

V. SUMMARY AND CONCLUSIONS

We considered local polariton states associated with pointlike defects in an isotropic dipole-active medium. The frequency interval available for these states (Fig. 1) is extended from the top of the lower polariton band Ω_{\max}^2 to the bottom of the longitudinal phonon band. The local states arise at the bottom of the polariton gap for an infinitesimally small value of the impurity strength α . Our analysis shows that near Ω_{\max}^2 they are composed from the long-wavelength polaritons. The typical momentum of these polaritons, k_{\max} , defines the coherence length of the local states, $l_{\text{coh}} \sim a\beta^{-1/2}$. The separation of these states from the bottom of the gap, $\omega - \Omega_{\max}$, defines their localization radius, $l_{\text{loc}} \sim a\beta^{-1} \alpha^{-1} \Omega_0^2$. Despite the atomic size of a defect, both characteristic lengths are macroscopic.

Local polariton states present the well-known phonon states with the field corrections taken into account. ‘‘Weight’’ of these corrections decreases as α increases and

the state moves away from the bottom of the gap. A long-wavelength nature of the phenomenon allows us to analyze the ‘‘impurity-strength-driven’’ crossover between polariton and phonon local states. We found that the crossover takes place within the frequency interval of the order of $\Delta_{\perp}^{1/2} \sim \beta^{1/2} \Omega_0$. However, despite a small size of the crossover region, the photon-phonon coupling sets a limit on the width of the spectral gap allowing the same type of local states in the entire gap [Eq. (29)]. We estimated the critical width of the spectral gap and showed that, in the case of the isotopic defects, only light impurities support local states in ‘‘narrow’’ gaps.

In the isotropic model, the distinct features of the local polariton states can be attributed to the singularity of the DOS, $\rho(\omega^2) \propto (\Omega_{\max}^2 - \omega^2)^{-1/2}$. This singularity is caused by the long-wavelength polaritons and is generic for any dipole-active phonon mode with negative dispersion and isotropic spectrum. We show that a weak crystal anisotropy removes the singularity from the band boundary [Eq. (33)], however, it does not lead to a finite threshold for the local polariton states. We argue that the properties of the polariton states (caused by negative dispersion of the long-wavelength optical phonons) are insensitive to other physical factors contributing to the finite DOS at the band boundary. At the same time, elimination of the DOS singularity replaces the power-law relation [Eq. (13)] between the impurity strength and the separation of the local state from the band boundary $\alpha \propto (\omega - \Omega_{\max})^{1/2}$ with the logarithmic relation $\alpha \propto -1/\ln(\omega - \Omega_{\max})$. Since our results are obtained in the long-wavelength approximation, the state must lie close enough to Ω_{\max} in order to ensure a macroscopic localization radius. On the other hand, if ω is too close to Ω_{\max} , quantum fluctuations can destroy the state. However, an analysis of these effects exceeds the limits of this paper and will be done elsewhere.

In the presence of a macroscopic concentration of impurities, the local states can provide the transmission inside the spectral gap. Since l_{loc} greatly exceeds l_{coh} , the transmission regime critically depends on the impurity concentration n . When $n^{-1/3} \ll l_{\text{loc}}$, an exponentially small tunneling probability corresponds to a localized regime. For $l_{\text{loc}} \sim n^{-1/3}$, the resonant tunneling of excitations from one impurity to another gives rise to a diffuse propagation of the radiation. When $n^{-1/3}$ approaches l_{coh} , the impurity band begins to form, and the transmission regime regains properties of the coherent propagation. Due to a macroscopic value of l_{coh} , this should occur at a very low concentration of impurities $na^3 \geq \beta^{3/2}$.

Local polariton states provide a ‘‘phonon-assisted localization’’ of electromagnetic waves. However, our estimates show a strong suppression of the photon content of these states, $W_{\text{phot}}/W_{\text{phon}} \sim \beta$. This is caused by the fact that k_{\max} is much greater than the crossing-resonance momentum k_0 . To eliminate this disproportion, one needs to lower the group velocity of electromagnetic waves in the active medium. This can be achieved in an active medium inside a narrow waveguide. For instance, the dispersion law of the modes propagating in the parallel-plate waveguide, $\omega/c = \sqrt{(\pi n/l)^2 + k^2}$, provides the reduction of their group velocity in the long-wavelength region. Preliminary estimates show that for $l \sim 10^6 a$ the phonon and photon velocities be-

come comparable in the crossing-resonance region. The detailed analysis of a possibility of photon localization in thin dipole-active films will be presented elsewhere.

ACKNOWLEDGMENTS

I wish to thank L. I. Deych and A. A. Lisiansky for useful discussions and comments on the manuscript. This work was supported by a CUNY collaborative grant.

APPENDIX

In order to evaluate the transverse integral in Eq. (6), we present $I_{\perp}(\omega^2)$ as a sum of two terms by separating the Brillouin zone into two parts:

$$I_{\perp}(\omega^2) = \frac{2}{3} \left(\frac{a}{2\pi} \right)^3 \int d\mathbf{k} \left(\omega^2 - \Omega_{\perp}^2 - \frac{d^2 \omega^2}{\omega^2 - c^2 k^2} \right)^{-1} = I'_{\perp}(\omega^2) + I''_{\perp}(\omega^2). \quad (\text{A1})$$

The first term, $I'_{\perp}(\omega^2)$, involves integration over $k < k'_0$ including the crossing-resonance region, and $I''_{\perp}(\omega^2)$ presents the integral over the remaining part of the Brillouin zone $k > k'_0$. The separating momentum k'_0 is convenient to fix by the condition $\Omega_{\perp}^2(k'_0) = \Omega_{\max}^2$ (Fig. 1).

Since k'_0 is located far away from the crossing-resonance point, the product ck in $I''_{\perp}(\omega^2)$ greatly exceeds the typical phonon frequencies and there we can set $ck = \infty$

$$I''_{\perp}(\omega^2) = \frac{2}{3} \left(\frac{a}{2\pi} \right)^3 \int_{k > k'_0} \frac{d\mathbf{k}}{\omega^2 - \Omega_{\perp}^2} = \frac{2}{3} \int_{\Omega_0^2 - \Delta_{\perp}}^{\Omega_{\max}^2} \frac{\rho_{\perp}(\varepsilon) d\varepsilon}{\omega^2 - \varepsilon}. \quad (\text{A2})$$

Using Eq. (22) for $\rho_{\perp}(\varepsilon)$, we can calculate the last integral

$$I''_{\perp}(\omega^2) = \frac{16}{3\pi\Delta_{\perp}} [(2\delta - 1) \arcsin \sqrt{\delta_1 - \sqrt{\delta_1(1 - \delta_1)}} + \sqrt{\delta|1 - \delta|} F(\omega^2)], \quad (\text{A3})$$

where

$F(\omega^2)$

$$= \begin{cases} + \ln \frac{\sqrt{\delta(1 - \delta_1)} + \sqrt{\delta_1(1 - \delta)}}{\sqrt{\delta(1 - \delta_1)} - \sqrt{\delta_1(1 - \delta)}} & \text{for } \Omega_{\max}^2 \leq \omega^2 \leq \Omega_0^2 \\ - 2 \arctan \sqrt{\frac{\delta_1(\delta - 1)}{\delta(1 - \delta_1)}} & \text{for } \omega^2 \geq \Omega_0^2, \end{cases} \quad (\text{A4})$$

and we denote $\delta_1 = (\Delta_{\perp} - \Delta_1)/\Delta_{\perp}$, and $\delta = (\Delta_{\perp} + \omega^2 - \Omega_0^2)/\Delta_{\perp}$.

The second term in Eq. (A1) includes integration over the crossing-resonance region where the polariton effects cannot be neglected. Recalling that $I'_{\perp}(\omega^2)$ presents the integral over the long-wavelength modes and using Eqs. (4) and (20), we can rewrite $I'_{\perp}(\omega^2)$ in the form

$$I'_{\perp}(\omega^2) = \frac{2}{3} \int_{\Omega_{\max}^2}^{\Omega_0^2} \frac{(\Omega_0^2 - \varepsilon) \rho_{\perp}(\varepsilon) d\varepsilon}{(\varepsilon - \omega^2)(\varepsilon - \Omega_0^2) + (\omega d v/c)^2} = \frac{16\Delta_1}{3\pi\Delta_{\perp}^2} \int_0^1 \frac{x^{3/2}(b-x)^{1/2} dx}{(x-a_+)(x-a_-)}. \quad (\text{A5})$$

Here $b = \Delta_{\perp}/\Delta_1$ is a large parameter, and two poles of the integrand are given by the equation

$$a_{\pm} = \frac{1}{2\Delta_1} [\Omega_0^2 - \omega^2 \pm (\omega^2 - \omega_-^2)^{1/2} (\omega^2 - \omega_+^2)^{1/2}], \quad (\text{A6})$$

where $\omega_{\pm}^2 = \Omega_0^2 \pm \Delta_1$, so that ω_-^2 coincides with the bottom of the gap Ω_{\max}^2 .

In the interval $\omega_-^2 \leq \omega^2 \leq \omega_+^2$, where a_{\pm} are complex-valued, we obtain

$$I'_{\perp}(\omega^2) = \frac{16\Delta_1^{1/2}}{3\pi\Delta_{\perp}^{3/2}} \left[2 + \frac{\nu^2 - 3\eta^2}{2\eta} \left(\arctan \frac{1 - \nu}{\eta} + \arctan \frac{1 + \nu}{\eta} \right) + \frac{3\nu^2 - \eta^2}{4\nu} \ln \frac{(1 - \nu)^2 + \eta^2}{(1 + \nu)^2 + \eta^2} \right], \quad (\text{A7})$$

where the parameters ν and η are defined by the equations

$$\nu^2 - \eta^2 = \frac{\Omega_0^2 - \omega^2}{2\Delta_1}, \quad (\text{A8})$$

$$2\nu\eta = \frac{(\omega_+^2 - \omega^2)^{1/2} (\omega^2 - \omega_-^2)^{1/2}}{2\Delta_1}. \quad (\text{A9})$$

For $\omega^2 \geq \Omega_0^2 + \Delta_1$, where a_{\pm} are negative, Eq. (A5) leads to

$$I'_{\perp}(\omega^2) = \frac{32\Delta_1^{1/2}}{3\pi\Delta_{\perp}^{3/2}} \left(1 - \frac{|a_+|^{3/2} \arctan|a_+|^{-1/2} - |a_-|^{3/2} \arctan|a_-|^{-1/2}}{|a_+| - |a_-|} \right). \quad (\text{A10})$$

Further straightforward analysis of the asymptotes of $I'_{\perp}(\omega^2)$ leads to Eqs. (23)–(25).

- ¹A.Z. Genack, Phys. Rev. Lett. **58**, 2043 (1987); M. Drake and A.Z. Genack, *ibid.* **63**, 259 (1989).
- ²S. John, Phys. Rev. Lett. **53**, 2169 (1984); Phys. Rev. B **31**, 304 (1985).
- ³K. Arya, Z.B. Su, and J.L. Birman, Phys. Rev. Lett. **57**, 272 (1986).
- ⁴T.R. Kirkpatrick, Phys. Rev. B **31**, 5746 (1985); C.A. Condat and T.R. Kirkpatrick, Phys. Rev. Lett. **58**, 226 (1987).
- ⁵*Scattering and Localization of Classical Waves in Random Media*, edited by Ping Sheng (World Scientific, Singapore, 1990).
- ⁶E. Yablonovich, Phys. Rev. Lett. **58**, 2059 (1987); E. Yablonovich and T.J. Gmitter, *ibid.* **63**, 1950 (1989).
- ⁷S. John, Phys. Rev. Lett. **58**, 2486 (1987); S. John and R. Rangarajan, Phys. Rev. B **38**, 10 101 (1988); S. John and T. Wang, Phys. Rev. Lett. **64**, 2418 (1990); Phys. Rev. B **43**, 12 772 (1991).
- ⁸*Photonic Band Gaps and Localization*, edited by C. M. Soucoulis (Plenum Press, New York, 1993).
- ⁹V.I. Rupasov and M. Singh, Phys. Rev. Lett. **77**, 338 (1996); Phys. Rev. A **56**, 898 (1997).
- ¹⁰S. John and V.I. Rupasov, Phys. Rev. Lett. **79**, 821 (1997).
- ¹¹L.I. Deych and A.A. Lisyansky, Phys. Lett. A **4**, 340 (1998).
- ¹²A. A. Maradudin, I. M. Lifshits, A. M. Kosevich, W. Cochran, and M. J. P. Musgrave, *Lattice Dynamics* (Benjamin, New York, 1969).
- ¹³A. A. Maradudin, E. W. Montroll, G. H. Weiss, and I. P. Ipatova, *Theory of Lattice Dynamics in the Harmonic Approximation* (Academic Press, New York, 1971).
- ¹⁴V.S. Podolsky, L.I. Deych, and A.A. Lisyansky, Phys. Rev. B **57**, 5168 (1998).
- ¹⁵A. Figotin and A. Klein (unpublished).